ChemPubSoc Europe

DOI: 10.1002/chem.201903141

CHEMISTRY A European Journal Full Paper

Crystal Field Theory

Derivation of Lanthanide Series Crystal Field Parameters From First Principles

Julie Jung,[a] M. Ashraful Islam,[b] Vincent L. Pecoraro,[c] Talal Mallah,[d] Claude Berthon,[e] and Hélène Bolvin*[b]

Abstract: Two series of lanthanide complexes have been chosen to analyze trends in the magnetic properties and crystal field parameters (CFPs) along the two series: The highly symmetric $LnZn_{16}(picHA)_{16}$ series (Ln = Tb, Dy, Ho, Er, Yb; picHA = picolinohydroxamic acid) and the $[Ln(dpa)_3](C_3H_5N_2)_3{\cdot}3H_2O$ series (Ln = Ce–Yb; dpa = 2,6-dipicolinic acid) with approximate three-fold symmetry. The first series presents a compressed coordination sphere of eight oxygen atoms whereas in the second series, the coordination sphere consists of an elongated coordination sphere formed of six oxygen atoms. The CFPs have been deduced from ab initio calculations using two methods: The AILFT (ab initio ligand field theory) method, in which the parameters are determined at the orbital level, and the ITO (irreducible tensor operator) decomposition, in which the problems are treated at the many-electron level. It has been found that the CFPs are transferable from one derivative to another, within a given series, as a first approximation. The sign of the second-order parameter B_0^2 differs in the two series, reflecting the different environments. It has been found that the use of the strength parameter *S* allows for an easy comparison between complexes. Furthermore, in both series, the parameters have been found to decrease in magnitude along the series, and this decrease is attributed to covalent effects.

Introduction

With the discovery of lanthanides as single-ion magnets,[1] there has been a resurgence of activity in the synthesis of new lanthanide complexes. Crystal field (CF) theory has been widely used to rationalize the properties of these complexes, in particular the nature of the ground state and the anisotropy of the magnetic properties. Crystal field parameters (CFPs) play a key role in the modeling of paramagnetic (pNMR) shifts in lanthanide complexes, according to the theory proposed by Bleaney in the 1970s. CF theory models the splitting of the metal orbitals, either d or f, in the presence of the ligands.[2] First proposed for the d elements in transition-metal complexes as a pure electrostatic interaction,[3,4] Racah and Stevens applied the Wigner–Eckart theorem to simplify the evaluation of the CF matrix elements for many-electron cases.[5,6] Since then, the formalism has been extended to the f elements.[7] It provides a theoretical framework for modeling the ion environment by means of a few parameters. CFPs are considered as phenomenological parameters, and are fitted against experimental data.

For lanthanide-containing complexes, the interaction between the lanthanide ion and the ligands has always been considered to be mostly electrostatic in nature. The nature of the ground state has been, therefore, rationalized by using electrostatic arguments; two software packages, CONDON and PHI, were developed for an efficient fitting of the CFPs against experimental data.[8,9] On an electrostatic basis and for highly symmetrical molecules, Rinehart and Long have shown that the shape of the ligand environment allows the nature of the low-lying M_J states to be predicted and thus the magnetic behavior of the complexes.[10] This model holds in a high-symmetry environment. To describe less symmetrical environments, computational approaches have recently been proposed that 1) combine an electrostatic description with semi-empirical radial effective charges (RECs)[11] and 2) describe the ligands by charges either optimized to fit the experimental data within the lone-pair effective charge (LPEC) model[12] or taken from ab initio calculations (CAMMEL).[13] A purely electrostatic approach has been proposed to determine the direction of the magnetic moment by minimizing the potential energy; the ligands are

[a] *Dr. J. Jung*
Theoretical division, Los Alamos National Laboratory
Los Alamos, New Mexico 87545 (USA)

[b] *M. A. Islam, Dr. H. Bolvin*
Laboratoire de Chimie et Physique Quantiques, CNRS
Université Toulouse III, 118 route de Narbonne, 31062 Toulouse (France)
E-mail: bolvin@irsamc.ups-tlse.fr

[c] *Dr. V. L. Pecoraro*
Department of Chemistry, Willard H. Dow Laboratories
University of Michigan, Ann Arbor, Michigan, 48109 (USA)

[d] *Dr. T. Mallah*
Institut de Chimie Moléculaire et des Matériaux d'Orsay, CNRS
Université de Paris-Sud 11, 91405 Orsay Cedex (France)

[e] *Dr. C. Berthon*
CEA, Nuclear Energy Division, Radiochemistry Processes Department
DRCP, BP 17171, 30207 Bagnols sur Cèze (France)

Supporting information and the ORCID identification number(s) for the author(s) of this article can be found under: https://doi.org/10.1002/chem.201903141.

modeled by fractional charges determined by valence-bond resonance hybrids.[14]

Even though the lanthanide-ion–ligand interaction is predominately electrostatic, some degree of covalency has been evidenced, but to a lesser extent than for the 5f elements. The 5d and 6s orbitals participate the most in the mixing, due to the inner-shell character of the 4f orbitals.[15–17] First-principles calculations allow for an accurate description of bonding, describing correctly both electrostatic and the tiny covalent bonding effects. They have become a useful tool to interpret the magnetic data of lanthanide complexes, by providing the nature of the ground state and the associated magnetic moment as well as the nature of the low-lying states that may be involved in relaxation processes,[18] and are a useful support for the interpretation of experimental data relating to lanthanide complexes.[19] More recently, ab initio calculations have also been successful in describing the magnetic coupling between two lanthanide centers.[20] Magnetic anisotropy is modeled by the so-called *g* tensor and the splitting of the ground manifold by the ligands in the absence of a magnetic field by the zero-field splitting (ZFS) tensor. These model parameters can be obtained from fitting experimental data with a model Hamiltonian, and from ab initio calculations.[21,22] In transition-metal complexes, the ZFS is induced by the spin–orbit coupling with excited states,[23] whereas in the f elements it arises from the splitting of the ground *J* multiplet of the free ion by the ligands and is characterized by the CFPs. In principle, the ZFS needs 27 independent parameters, although this number is reduced by symmetry. For example, in octahedral symmetry, only two CFPs are left, and they are easily deduced from both experimental data and calculation by fitting the energies of the states.[24] For lower symmetry, the number of CFPs increases, and at some point it is no longer possible to evaluate these parameters, either from experimental data or from the computed energies of the levels. However, all the information is available from ab initio calculations and two methods have recently been proposed for this purpose.

The aim of this work was to analyze the correlations between structure and the CFPs deduced from ab initio calculations, as well as the expected magnetic properties according to their prolate or oblate shape in two series of lanthanide complexes. The advantage of using ab initio calculations is three-fold: 1) All types of interactions are taken into account, not only the electrostatic interactions, 2) the 27 CFPs can be determined in the case of low symmetry, and 3) the relevance of CF theory to the modeling of the low-lying spectrum can be assessed. In the first series, denoted $LnZn_{16}$, the lanthanide ion is sandwiched between metallacrown species to form a quasi-perfect compressed D_{4d} symmetry, which reduces the number of CFPs.[25–27] This is a rare case in which the qualitative electrostatic model of Rinehart and Long applies almost perfectly.[10] The second series, denoted $[Ln(dpa)_3]^{3-}$, covers the whole period, the environment is more prolate, and the complexes show close to three-fold symmetry, but not strictly.[28] As will appear from the calculations, the magnetization stays axial along the series with a variation in the direction. Furthermore, the second-order parameter was recently deduced from paramagnetic NMR spectroscopy, applying Bleaney's theory.[28]

The CFPs were deduced from ab initio calculations by using different methods and the results have been compared. The CFPs were determined from the energy matrix derived from either the basis sets of the orbitals (ab initio ligand field theory, AILFT)[29] or the basis set of the many-electron wave functions (irreducible technique operator, ITO).[30] Because the first series is highly symmetrical, the CFPs could be directly fitted against the energies. This work completes a previous study in which another question about CFPs was addressed, namely the transferability of the CFPs from the orbital picture to the many-electron picture, including spin–orbit coupling. It emerged from this previous study that covalent effects between the metal and the ligands affect the CFPs, even for the ionic $PrCl_3$ crystal.[31] This will be confirmed by the present work in which we aimed to address the following points: 1) Do the two above-mentioned methods provide similar CFPs? 2) Are the CFPs transferable within each series as they depend only on the nature and position of the ligands? 3) How to connect the CFPs to the magnetic properties? 4) Are the trends across the series impacted by covalent effects?

In this report the two series are described first, the main features of the methods for the determination of the CFPs from ab initio calculation are then presented, with more details provided in the Supporting Information (Sections S1 and S2), and finally, the results of the CFP calculations for the two series mentioned above and the trend in the computed CFPs are discussed.

Two lanthanide series

$LnZn_{16}$

The isostructural $LnZn_{16}(picHA)_{16}$ (Ln = Tb, Dy, Ho, Er; picHA = picolinohydroxamic acid) series of compounds were synthesized by Pecoraro and co-workers and characterized by magnetometry.[25,27] This series has been completed by $YbZn_{16}(pyzHA)_{16}$ (pyzHA = pyrazinecarbohydroxamic acid), which is isostructural with $LnZn_{16}(picHA)_{16}$ and possesses attractive near-infrared (NIR) emission properties.[26] The structures of the lighter lanthanides, when available, are structurally different due to the presence of water molecules in the coordination sphere. In this series, two 12-MC-4 (MC = metallacrown) sandwich the Ln^{III}, and a further 24-MC-8 ring lies around this sandwich as a result of π-stacking interactions with the picHA rings (see Figure 1). The Ln^{III} are surrounded by eight oxygen atoms forming a compressed square antiprism geometry with very close to a perfect D_{4d} symmetry. The Ln–O distance ranges from 2.35 (Tb) to 2.31 Å (Yb) following the diminution of the ionic radius across the series. The angle with the quaternary axis is constant and about 62.3°, which denotes a compressed environment. As described in Refs. [26,27], this compressed environment leads to unusual magnetic properties, with axial and planar magnetization for the Er^{III} and Dy^{III} complexes, respectively.

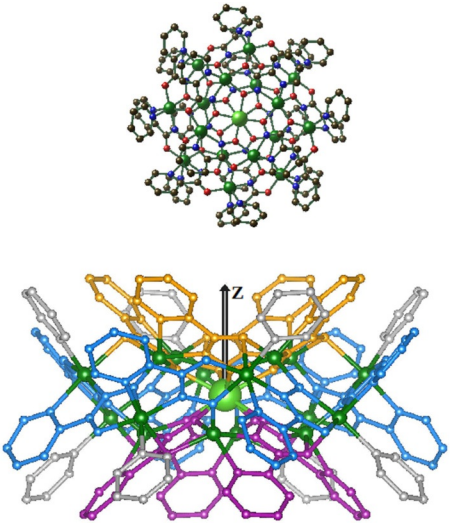

Figure 1. Structure of the $LnZn_{16}$ complexes.[25] Top: Top view, green: Er, Zn; red: O; blue: N; black: C. Bottom: Side view, purple: upper 12-MC-4; orange: lower 12-MC-4; blue: 24-MC-8 ring; grey: pyridine. Hydrogen atoms have been omitted for clarity.

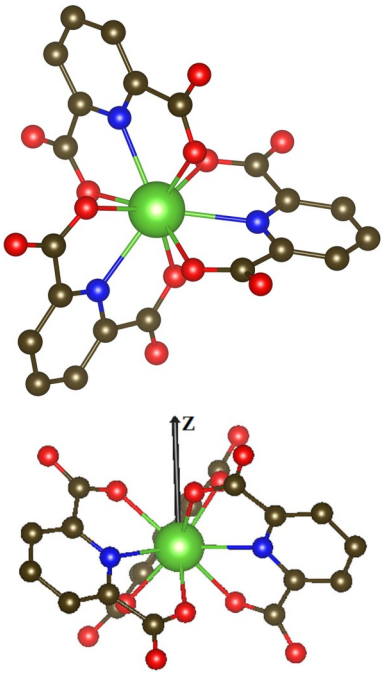

Figure 2. $[Ln(dpa)_3]^{3-}$ complex. Top: Top view. Bottom: Side view, green: Ln; red: O; blue: N; black: C. Hydrogen atoms have been omitted for clarity.

[Ln(dpa)$_3$]$^{3-}$

The $[Ln(dpa)_3](C_3H_5N_2)_3{\cdot}3H_2O$ (denoted $[Ln(dpa)_3]^{3-}$; Ln = Ce–Yb; dpa = 2,6-dipicolinic acid) series of compounds are also isostructural. The complexes have been structurally characterized by X-ray diffraction, except praseodymium, and crystallize in the triclinic space group *P*1.[28] The coordination sphere contains three DPA^{-} that form a distorted tricapped trigonal prism (see Figure 2). Each ligand is tridentate and coordinated to the Ln^{III} cation through the nitrogen atom of the pyridine cycle (capped position) and an oxygen atom of each of the carboxylate groups (prism position). The coordination sphere is formed by six oxygen and three nitrogen atoms with distances ranging from 2.51 (Ce–O) to 2.37 Å (Yb–O), and 2.63 (Ce–N) to 2.45 Å (Yb–N), respectively. Due to the presence of counter ions, the ternary symmetry is slightly distorted and, for a given complex, the distances between the metal ion and the three ligands differ by about 0.1 Å. The oxygen atoms are closer than the nitrogen ones, and are more electronegative, as confirmed by the Mulliken charges of around −0.9 and −0.2, respectively. One might expect the oxygen atoms to dominate the crystal field. The angle between the oxygen atoms and the pseudo-ternary axis is rather constant along the series at around 46°; this is a much smaller value than in the $LnZn_{16}$ series and denotes a prolate environment.

The whole $[Ln(dpa)_3]^{3-}$ series is considered in this work, except the gadolinium complex, which has a pure spin ground state and in which the ZFS arises from second-order interactions. The *Z* axis is perpendicular to the plane formed by the three nitrogen atoms, whereas the *X* and *Y* axes are arbitrary (see Figure 2).

Crystal field parameters

Model Hamiltonian within crystal field theory

The Hamiltonian describing the f electrons may be written as Equation (1)

$$\hat{\mathcal{H}}^{CF} = \sum_{i=1}^{N}\left[\hat{T}_i - \frac{Z^*}{r_i}\right] + \sum_{i<j}\frac{1}{r_{ij}} + \sum_{i=1}^{N}\left[\hat{\xi}\hat{l}_i\hat{s}_i + \hat{v}^{CF}(r_i)\right] \quad (1)$$

with the scalar relativistic kinetic term, the attraction of the electrons by the screened charge of the metal nucleus *Z**, the electron–electron repulsion, the spin–orbit operator, and the one-electron CF operator, respectively. The sum runs over the *N* f electrons of the valence shell. The many-electron CF operator is the sum of the one-electron operators given by Equation (2)

$$\hat{V}^{CF} = \sum_{i=1}^{N}\hat{v}^{CF}(r_i) \quad (2)$$

in which $\hat{v}^{CF}$ is the electrostatic potential at a point *r* close to the magnetic center arising from the ligands represented by point charges. In its pure electrostatic formulation, it arises from the charges attributed to the ligands and it is written as a multipolar expansion in terms of spherical coordinates [Eq. (3)].

$$\hat{v}^{CF}(r) = \sum_{k=0}^{\infty}\sum_{q=-k}^{k} b_k^q r^k Y_k^q(\theta,\phi) = \sum_{k,q}\hat{v}_k^q(r) \quad (3)$$

The term $\widehat{v}_k^q(r)$ represents components of irreducible tensors of rank k, and their matrix elements within an f^N configuration with pure f orbitals vanish for $k>6$ as well as for odd values of k. The first term, with $k=0$, does not contribute to CF splitting.[32] The noncontributing terms (k, q) are usually omitted in the expansion of Equation (3), and the number of terms is further reduced by symmetry.

Assuming that all the 4f orbitals have the same spatial expansion, the $\widehat{v}_k^q$ operators (or their many-electron counterparts) acting in the Hilbert space of the Slater determinants may be replaced by the tensor operators $\widehat{O}_k^q$ acting in either the l (one-electron), L (spin-free), or J (spin–orbit) manifolds. Equation (2) is then equivalent to Equation (4)

$$\widehat{V}^{CF}(X) = \sum_{k=2,4,6} \alpha_X^k \sum_{q=-k}^{k} B_q^k \widehat{O}_q^k(X) \tag{4}$$

in which $X = l, L, J$ according to the considered manifold. The term $\alpha_X^k = \langle X \| \alpha^k \| X \rangle$ represents the reduced matrix elements of the second, fourth, and sixth order, respectively. The α_l^k elements are determined by N, the α_L^k elements by N and L, and the α_J^k elements by N, L, and J. These reduced matrix elements have been tabulated for the ground state of each lanthanide ion.[32] The convention of Wybourne is used throughout this work.[7,33] It was understood very early on that the pure electrostatic picture is far from quantitative. Because the incorporation of some covalency keeps the one-electron structure, $\widehat{V}^{CF}$ may be seen as an effective interaction, the parameters of which are fitted on experimental data. We showed in a recent article[31] that the CFPs deduced from orbital energies ($X=l$) and from many-electron wave functions without or with spin–orbit coupling ($X=L$ and J, respectively) lead to similar CFPs. Consequently, the reduced elements α_X^k depend on the nature of the metal, and the CFPs B_q^k only on the nature and position of the ligands, and should be transferable within the lanthanide series.

The CFPs depend on the orientation of the molecule in the {X, Y, Z} frame. They are in general imaginary, and rotations around the Z axis affect the phase factor mixing B_q^k and B_{-q}^k. In the present work, Z was chosen as the pseudo-rotation axis (cf. Figure 1 and Figure 2), and the choice of X and Y axes is arbitrary. Hence, only the norm of these parameters is considered in this article[34] [Eq. (5)].

$$\overline{B}_q^k = \sqrt{\left|B_q^k\right|^2 + \left|B_{-q}^k\right|^2} \tag{5}$$

For the sake of comparison, rotational invariants are considered to reduce the numerous CFPs to fewer parameters, more specifically the second-order moments.[35,36] We considered the strength parameter of kth order [Eq. (6)]

$$S^k = \left[\frac{1}{2k+1}\sum_{q=-k}^{k}\left|B_q^k\right|^2\right]^{1/2} \tag{6}$$

and the strength parameter as defined by Chang et al.[35] [Eq. (7)].

$$S = \left[\frac{1}{3}\sum_{k}\frac{1}{2k+1}\sum_{q=-k}^{k}\left|B_q^k\right|^2\right]^{1/2} \tag{7}$$

These two strength parameters are rotational invariant. To quantify the symmetry about the Z axis, the strength parameter of qth index was considered [Eq. (8)].

$$S_q = \left[\sum_{k}\frac{1}{2k+1}\left|B_q^k\right|^2\right]^{1/2} \tag{8}$$

This parameter is not rotational invariant, but it is invariant to rotations about the Z axis. Equations (6), (7), and (8) are related by Equation (9).

$$S = \sqrt{\frac{S^2+S^4+S^6}{3}} = \sqrt{\frac{S_0+S_1+S_2+S_3+S_4+S_5+S_6}{3}} \tag{9}$$

The parameter S allows the strength of the ligand field to be evaluated with only one parameter and gives an idea of the overall splitting of the ground J manifold.

Crystal field parameters from first principles

The CFPs model the splitting of a J multiplet of the free ion by the ligands, and according to CF theory, there are 27 such parameters. The CF operator of Equation (3) is essentially a one-electron operator that acts at the orbital level. By applying the Wigner–Eckart theorem, it may be expressed as a many-electron operator acting in a given J manifold [Eq. (4)].[5,6] In transition-metal complexes, the ZFS arises due to spin–orbit coupling with excited states, and the analysis at the orbital level needs symmetry considerations;[37] in lanthanide complexes, CFPs determined at the orbital or many-electron levels are similar, because the splitting of the 4f orbitals by the CF is sufficiently small not to impact the composition of the many-electron wave functions of the free ion.[31] Once the CFPs are known, the energies and compositions of the $2J+1$ states arising from this manifold are fully characterized, and all the magnetic and spectroscopic properties may be deduced.

Ab initio calculations based on the CASSCF (complete active space self-consistent field) method provide the energies of the low-lying states and their compositions in terms of Slater determinants, which provide the necessary information for the determination of the CFPs. In the AILFT method developed by Atanasov et al., the CF operator in its one-electron picture is considered, and additional parameters are needed to model the two-electron interaction (Slater–Condon parameters) and the spin–orbit interaction.[29] On the other hand, in the ITO method proposed by Ungur and Chibotaru, the CF operator in its operator-equivalent picture is considered, and the CFPs are deduced from the many-electron energies and wave functions

of the considered J manifold.[30] The determination of spin Hamiltonian parameters from ab initio calculations needs the one-to-one correspondence between the computed and model states, and this is usually a key stage of the procedure.[22,38,39] For AILFT, the correspondence is performed at the one-electron level by mapping the seven 4f orbitals, whereas for ITO, it is performed by determining the eigenvectors of the magnetic moment operators. Finally, in the AILFT method the CFPs are deduced from a fitting procedure, whereas in the ITO method a decomposition is performed by using the irreducible tensor operator technique.

Fitting procedure (FIT)

In the case of complexes with high symmetry, the number of CFPs is reduced. In octahedral symmetry, there are two independent parameters[40] and the CFPs are easily deduced from ab initio calculations.[24] When an axial symmetry is present, there are only three CFPs left: B_0^2, B_0^4, and B_0^6. In this case, the parameters can be fitted against the ab initio energies by a least-squares procedure when J is large enough. Then, the states are assigned according to the projection of the total angular moment $\widehat{J}_Z$. This method was applied to the $LnZn_{16}$ series, which evidence a symmetry very close to D_{4d}. This is still feasible when a few off-diagonal terms are present ($q \neq 0$), as for D_{3h} with an additional B_6^6 term.[31]

Ab initio ligand field theory (AILFT)

The second approach was developed by Atanasov et al.,[29] first based on DFT calculations[41] and afterwards adapted to wavefunction theory (WFT).[42] It has been applied to octahedral series of lanthanides[43] and actinides.[44] The many-electron wave functions of a $4f^N$ ion are written as linear combinations of Slater determinants $|\varphi_i \cdots \varphi_j|$ built with real 4f spin orbitals φ_i. Because 4f orbitals are very inner shell, the φ_i are almost of pure 4f character. The correspondence with the model space is performed at this stage. Both the ab initio and the model Hamiltonians of Equation (1) are expanded in the Slater determinants basis, and there is a one-to-one correspondence of the matrix elements. The model matrix is expressed by the 27 CF matrix elements, the three Slater–Condon parameters for electron–electron repulsion F^2, F^4, and F^6,[45] and the effective one-electron spin–orbit coupling parameter ξ. These parameters are deduced by equating the matrix elements of the ab initio and model matrices. The system of equations is overparametrized, and is solved through a least-squares procedure. More details are given in Section S1 in the Supporting Information.

Irreducible tensor operator (ITO) method

This method has been proposed by Ungur and Chibotaru.[30] The CFPs are deduced from the $2J+1$ wave functions and the corresponding energies of a J term of the free ion. This assumes that this manifold is well separated from the other ones and easily identifiable. Because the ab initio eigenvectors of the Z component of the total angular magnetic moment $\widehat{M}_Z$ correspond to the $\{|J, M_J\rangle\}$ model vectors, the one-to-one correspondence is performed by diagonalizing the representation matrix of $\widehat{M}_Z$ in the J manifold. The phase factors between the states are further determined such that the superdiagonal of the representation matrix of $\widehat{M}_X$ is real. The ab initio Hamiltonian matrix is then expressed in this new basis set, and is decomposed in terms of the spin matrices of the ITOs.[46,47] The corresponding projections are the CFPs within the reduced matrix elements α_J^k of Equation (4). Because the CFPs are obtained by a decomposition technique, there is no loss of information, but the $2J+1$ degrees of freedom reduce naturally to 27: Although the odd-order parameters vanish because of time-reversal symmetry of the Hamiltonian, parameters with $k>6$ appear to be negligible. The similarity between the ab initio M_u^J and the model M_u^{AI} matrices in the direction u is quantified by the distance between these matrices, as given by Equation (10)

$$\delta m_u = \sqrt{\mathrm{Tr}\left(\boldsymbol{M}_u^J - \boldsymbol{M}_u^{AI}\right)^{\dagger}\left(\boldsymbol{M}_u^J - \boldsymbol{M}_u^{AI}\right)} \qquad (10)$$

in which $\dagger$ denotes the conjugate transpose. δm_u vanishes in the limit of the free ion in the LS coupling scheme. Another index, δh, is introduced to quantify the similarity between the ab initio and model Hamiltonian representation matrices [see Eq. (S8) in the Supporting Information]. More details are given in Section S2.

Results and Discussion

$LnZn_{16}$

The axial symmetry leads to a reduced number of CFPs, namely B_0^2, B_0^4, and B_0^6, which can be fitted either against the experimental data or ab initio results. In this work we compared the CFPs determined from ab initio calculations with those derived from both the FIT and ITO methods. The CFPs obtained for the five complexes are summarized in Table S1 in the Supporting Information and are presented graphically in Figure 3. The energies of the ground J manifold are given in Table S2. The two methods lead to identical values. With ITO, due to a small twist angle around the Z axis slightly breaking the D_{4d} symmetry, some CFPs with $q \neq 0$ are non-zero, as for example B_4^4 and B_4^6.

B_0^2 is the largest in magnitude, and negative as expected from a compressed environment. This negative value of B_0^2 leads the magnetization to be axial in the erbium derivative, and planar in the dysprosium derivative.[10,31] B_0^4 and B_0^6 are far from non-negligible, around $\pm 500\ \mathrm{cm}^{-1}$, and opposite in sign, which leads to entangled spectra in terms of $|M_J|$. As discussed in Ref. [31], α_J^2 changes sign between holmium and erbium. This impacts the ordering of the states in terms of $|M_J|$: For terbium and dysprosium, $|M_J|$ increases with the energy, for ytterbium, it decreases. For the holmium and erbium complexes, the states are more entangled due to the significant values of B_0^4 and B_0^6, which lead to a nonquadratic relation between the energy and $|M_J|$. All the CFPs decrease in

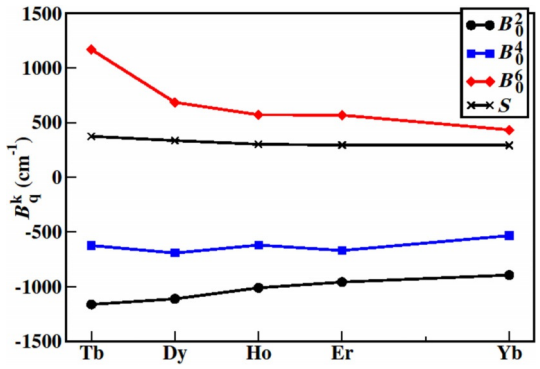

Figure 3. CFPs and strength parameters for the $LnZn_{16}$ series derived from the ITO method. For $HoZn_{16}$, the values are averaged over the $DyZn_{16}$ and $ErZn_{16}$ structures.

magnitude along the series, which will be further discussed in the last section, and consequently the strength parameter S, defined in Equation (7), follows this trend.

$[Ln(dpa)_3]^{3-}$

Because the real and imaginary parts of the nondiagonal CFPs vary by any rotation in the XY plane, only their norm is considered, $\overline{B}^k_q$, as defined in Equation (5). The CFPs were calculated by both AILFT and ITO. For ITO, the manifolds with $J<3$ do not provide sixth-order CFPs because the expansion of Equation (S5) (in the Supporting Information) is limited to $2J$. This artificially leads to smaller strength parameters S and S_q due to the restricted sum of terms [see Eqs. (7) and (8)]. To overcome this limitation, the sixth-order CFPs (and all orders for Eu^{III}) are deduced from the first excited J manifolds.

All the CFPs are given in Tables S6 and S7 in the Supporting Information, and the strength parameters in Tables S8 and S9. The dominant parameters are presented graphically in Figures 4 and 5, and the others are shown in Figures S2. The two methods give similar CFPs. This confirms that CFPs extracted from orbital and many-electron levels are very similar due to the small ZFS of the 4f orbitals. It should be mentioned that the energies of the low-lying excited states are very similar, even though they were calculated with different codes, different basis sets, and slightly different approximations (see Table S3). Although B^2_0, B^4_0, B^6_0, B^4_3, B^6_3, and B^6_6 have values of several hundred wavenumbers, all the other parameters are smaller than 100 cm^{-1}. This is in agreement with the approximate three-fold symmetry of the complexes. Indeed, within the trigonal C_3 point group, only these six CFPs would be nonzero. B^2_0 is positive, whereas B^4_0 and B^6_0 are negative, and all three CFPs are of the same order of magnitude. The sign of B^2_0 is opposite to that of the $LnZn_{16}$ series, which denotes a more prolate coordination environment. As in the other studied complexes, the CFPs are transferable along the series with an overall decrease in magnitude. This confirms that the effects of the ligands and central ion are decorrelated and independently described by the parameters B^k_q and α^k_j of Equation (4), respectively.

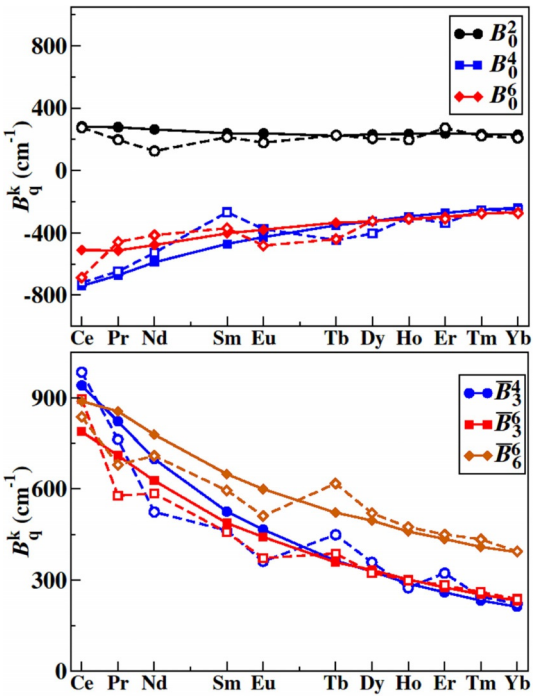

Figure 4. CFPs for the $[Ln(dpa)_3]^{3-}$ series. Full line: AILFT; dashed line: ITO.

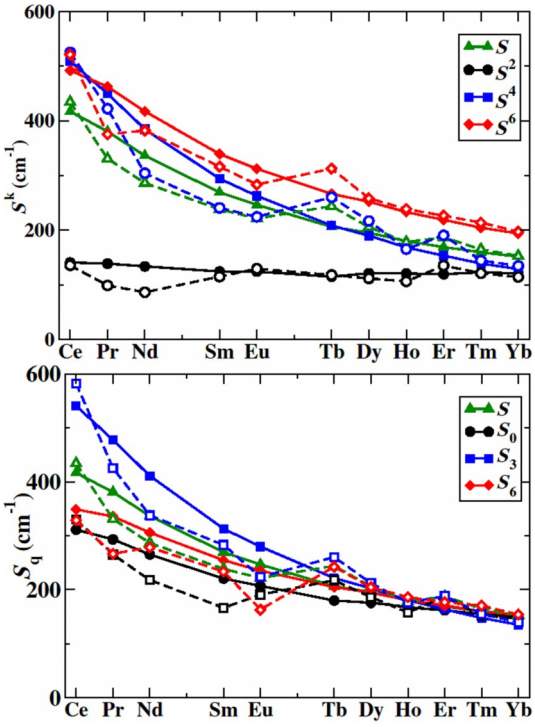

Figure 5. Strength parameters for the $[Ln(dpa)_3]^{3-}$ series. Full line: AILFT; dashed line: ITO.

In the case of complexes with axial symmetry, the nature of the ground-state magnetization alternates between planar and axial following the sign of α^2_j from Equation (4). In the $LnZn_{16}$ series, B^2_0 is negative, and the magnetization is planar for the dysprosium derivative and axial for the erbium one. For sand-

wich complexes,[31] B_0^2 is positive for benzene and cyclopentadienyl ligands and negative for the more compressed 1,3,5,7-cyclooctatetraene ligand, leading to opposite magnetic anisotropies for these different ligands. In the $[Ln(dpa)_3]^{3-}$ series, B_0^2 is positive as expected from the prolate layout of the oxygen atoms. Hence, one would expect a planar (axial) magnetization for samarium, erbium, and ytterbium (Ce, Nd, and Dy) due to a positive (negative) value of α_J^2. However, this is not the case, as can be seen from the *g* factors of the ground Kramers doublets given in Table S5. Because the fourth- and sixth-order CFPs, as well as the ternary nondiagonal parameters, are non-negligible, the ground states are far from pure M_J eigenstates. The dysprosium complex shows an axial magnetization, and so do the erbium and ytterbium complexes, with the magnetization in a direction perpendicular to the ternary axis. This is in agreement with previous observations:[48,49] In the presence of pseudo-axial symmetry, the magnetic anisotropy of elongated erbium derivatives, which is expected to be planar, is axial and oriented perpendicularly to the pseudo-axis. As a consequence, the magnetic axes of the dysprosium and erbium complexes are perpendicular.

Trends in the lanthanide series

Strength parameters and CFPs

The strength parameters are presented graphically for the two series in Figure 6 along with the metal–ligand distances. As discussed above, the strength parameter *S* defined by Equation (7) gathers in only one parameter the 27 CFPs and allows an easy evaluation of the strength of the metal–ligand interaction. This facilitates comparison between two complexes. Along the two series, the coordination sphere shrinks with the decrease in the ionic radius of the free ion. The CFPs decrease in magnitude along the two series and the value of *S* is larger for the $LnZn_{16}$ series than for $[Ln(dpa)_3]^{3-}$. In the pure electrostatic picture, according to Equation (3), the CFPs are determined by the position and charge of the ligands, as well as by the radial expansion of the 4f orbitals. Along the series, the nuclear charge of the lanthanide atom increases, the 4f orbitals become more inner shell, the ionic radius of the free ion decreases, and, accordingly, the coordination sphere shrinks. In an isostructural series, the structural changes are smooth and, as a first approximation, because they are determined only by the ligands, the CFPs may be considered as transferable from one lanthanide ion to another inside a series, as observed by Abragam and Bleaney.[32] The variation in the number of 4f electrons is included in the α_X^k reduced matrix elements, and the variation in α_X^k, both in amplitude and in sign, leads to very different energetic spectra and magnetic behavior from one lanthanide ion to another.

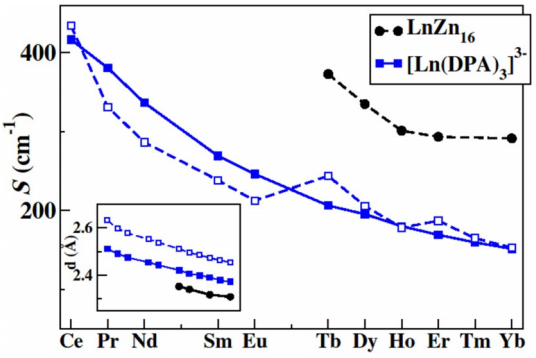

Figure 6. Strength parameters for the $LnZn_{16}$ and $[Ln(dpa)_3]^{3-}$ series. Full line: AILFT; dashed line: ITO. Insert: Average bond distances in the coordination sphere. $LnZn_{16}$: 8 oxygen atoms; $[Ln(dpa)_3]^{3-}$: full line: 6 oxygen atoms; dashed line: 3 nitrogen atoms.

Figure 6 shows a smooth variation of the CFPs; it can be said, as a first approximation, that they are transferable from one ion to the next with a small variation. But it may not be said that they are constant across the whole series. As was shown in Ref. [31], the trends in the many-electron spectra are much more tricky to analyze, because of the large variation in α_X^k, especially in α_X^2, the sign of which changes three times along the series. In the $LnZn_{16}$ series, except for B_0^6 the Tb^{III} complex, the three CFPs are rather constant, as they only decrease by 10–20% in magnitude (see Figure 3). δm_u, defined in Equation (10) with $u = X$, *Y*, and *Z* (see Table S1 in the Supporting Information), which quantifies the similarity of the $\hat{M}_u$ matrix to that of the free ion in the LS coupling scheme, decreases across the series to almost 0 for ytterbium. The same tendency is observed for δh [defined in Eq. (S8)], which quantifies the similarity of the ab initio and model matrices expanded up to the sixth order.

Point charge model

To analyze these variations, a point charge (PC) model has been considered in which each atom of the ligands is represented by a PC deduced from its LoProp ab initio value.[50] The electrostatic potentials created by the PC model and the ab initio ligands are similar (see Table S10 in the Supporting Information). The PC and ab initio strength parameters are compared in Figure 7. The PC strength parameter is rather constant across the series. Because the dipole and quadrupole moments determined by the two models are almost identical, the difference between the PC and ab initio calculations can be attributed to covalent contributions, including the combined effects of bonding, charge donation, and polarization. In the electrostatic model, the CF is axial and dominated by second-order terms (S^2 and S_0 dominant), and the other terms are almost negligible. This prevalence of the second order for electrostatic models has already been observed in $PrCl_3$ and sandwich complexes,[31] and it confirms that the nonaxial and fourth- and sixth-order contributions arise mostly from non-electrostatic effects such as the polarization of f orbitals, orthogonality issues, electron correlation, and covalent effects. As already mentioned, the PC model leads to a rather constant value of *S*. The difference between the ab initio and PC curves is rather constant for the second order, and tends to decrease for the fourth and sixth orders. It should be mentioned that a simplified PC model, in which the ligands are replaced by only nine point charges placed at the positions of the six oxygen and three nitrogen atoms of the coordination sphere, leads to re-

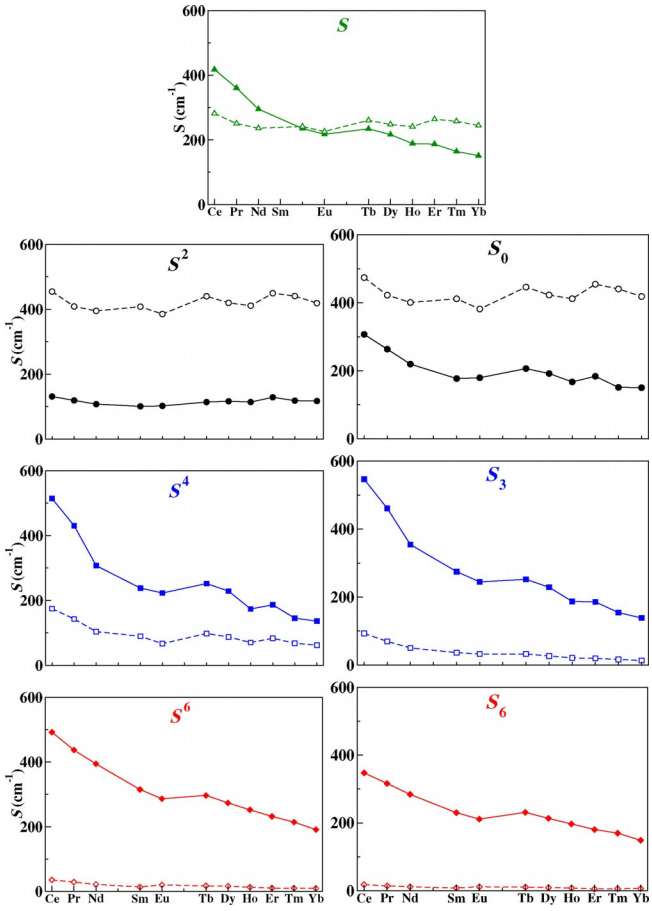

Figure 7. Strength parameters for the $[Ln(dpa)_3]^{3-}$ series determined by the ITO method. Full line: ab initio; dashed line: PC model.

sults similar to those obtained with the more sophisticated PC model (see Figure S6).

In the pure electrostatic picture, the closer the charges, then the greater the interactions and the CFPs. In the $LnZn_{16}$ series, the coordination sphere is more compressed than in the $[Ln(dpa)_3]^{3-}$ series, and S is larger because the ligands are closer to the 4f electrons. But the trend along a series is not so simple because there are two opposite effects: As the 4f orbitals contract, the CFPs should decrease, but as the coordination sphere shrinks, the CFPs should increase. To unravel these two effects, they were dissociated by varying independently the nature of the lanthanide ion and the position of the charges (see Section S4.5 in the Supporting Information). As expected, the CFPs decrease when changing the metal ion (fixed position of the point charges) and increase when changing the positions of the charges (fixed Ln). The contraction of the coordination sphere and the decrease in the spatial distribution of the 4f electrons lead to opposite trends along the series, and the interweaving effects lead to a rather constant value of S. Consequently, the decrease in the strength parameters observed in Figure 6 with the full ligands arises from the overlap of the lanthanide and ligand orbitals, namely covalent effects. The 4f orbitals being inner shell, they participate little in the covalent bonding itself, which involves mostly 5s, 5p, and 6d orbitals. It was shown in Ref. [31] that both the direct overlap of the 4f orbitals and the orbitals of the ligands and the indirect interaction of the more outer-shell orbitals affect the CFPs. As in this previous work, covalent effects reduce the CFPs of the second-order term and increase the other CFPs, and more specifically the off-diagonal terms with $q \neq 0$.

The decrease in the CFPs across the lanthanide series has been observed previously. Duan and Tanner fitted the energetic spectra of the whole series of $Cs_2NaLnCl_6$[51] taking advantage of the octahedral symmetry, which leads to only two non-vanishing independent CFPs. Both B_0^4 and B_0^6 decrease across the series, from 2100 (Ln = Ce) to 1400 cm^{-1} (Ln = Yb) and from 260 to 90 cm^{-1}, respectively. The authors showed that this decrease is larger than that expected for a pure PC model of the ligands. Faulkner et al.[52] improved the PC model by adding induced dipoles on to the ligands, and this led to a decrease in the CFPs. But the present work shows that the extended PC model leads to similar results to those obtained with the model with only nine PCs. Ishikawa et al. deduced the CFPs in the $[Pc_2Ln]^-$ series for the second part of the lanthanide series by fitting paramagnetic shifts and magnetic susceptibilities.[53] Both B_0^2 and B_0^4 decreased in magnitude whereas B_0^6 was rather constant, but small.

Comparison of ITO with AILFT

In the $[Ln(dpa)_3]^{3-}$ series, the variation in the CFPs along the series is smoother with AILFT than with ITO (see Figure 4). In the first half of the series, the ITO values are smaller than the AILFT values, whereas the opposite is observed in the second half. Also, there are more irregularities in the ITO values, especially in the first half of the series. In the first half, the value of J is small according to Hund's third rule, and the different J manifolds are closer to each other according to the Landé rule. It could be suspected that the spin–orbit coupling between the J manifolds is at the origin of these irregularities. The CFPs deduced before and after the inclusion of the spin–orbit coupling, within the L and J ground manifolds, respectively, are shown in Figure S4 in the Supporting Information. They are found to be very similar. This shows that the J–J coupling, which is more important at the beginning of the series, does not affect the CFPs. The model and ab initio magnetization matrices (see Table S4) differ more in the first half of the series, especially for neodymium and samarium. In the second half of the series, the values of δm are roughly the same as for the $LnZn_{16}$ series; they decrease and almost vanish for ytterbium. The highest values of δh are reached for neodymium and samarium, which means that orders higher than six are less negligible in these cases. The Slater–Condon parameters, which describe the electron–electron interaction, increase (see Figure S3). These trends show that the overlap of the metal and ligand orbitals, which is tiny, decreases across the series. Finally, the difference between the AILFT and ITO CFPs should be attributed to electron–electron effects. The former method determines the CFPs at the one-electron level, and the parameters for electron–electron repulsion and spin–orbit coupling are determined independently with additional parameters. In the ITO method, the CFPs are determined from the decompo-

sition of the many-electron wave functions and describe the other interactions in an effective way. It cannot be concluded that one approach is more reliable than the other: AILFT provides one-electron CFPs and, with the knowledge of Slater–Condon parameters and the SO coupling constant, the energies of all the states arising from the $4f^N$ configuration might be calculated. The ITO technique provides effective many-electron CFPs and is specific to each *J* manifold. For magnetic properties that arise only from the ground *J* manifold, the ITO method is recommended because they reproduce exactly the energies of this manifold, whereas for spectroscopic methods involving excited *J* manifolds, the AILFT approach is more suitable.

Paramagnetic NMR shifts

Another domain to which CFPs are successfully applied is the modeling of paramagnetic NMR shifts of lanthanide complexes. Bleaney has shown that the pseudo-contact contribution depends on B_0^2.[2] B_0^2 can be evaluated from pNMR shifts within the lanthanide series, assuming it is constant throughout the series (see Section S4.6 in the Supporting Information for more details). In Ref. [28], the pNMR shifts of the $[Ln(dpa)_3]^{3-}$ series were measured and modeled according to Bleaney's theory,[2] and B_0^2 was determined to be 51 with an arbitrary unit applying.[54] This corresponds to 62 cm^{-1}, as shown in Section S4.6 in the Supporting Information. This value is four times smaller than the value of 250 cm^{-1} obtained in this work. However, it should be noted that B_0^2 is almost constant across the series and is the only CFP showing this trend, which supports Bleaney's theory. It shows that Bleaney's B_0^2, which parametrizes the entire magnetic anisotropy in a single parameter, is not clearly related to the "true" B_0^2. It was recently pointed out by Vonci et al.[55] that B_0^2 is very sensitive to small structural variations.

Conclusion

CFPs have been extensively used to rationalize the properties of lanthanide complexes. Used as phenomenological parameters, they are fitted to experimental data, which is only possible for molecules of high symmetry, as this reduces the number of parameters and avoids overparametrization in the fitting procedure. With the success of lanthanide complexes as single-ion magnets, there is a need to better understand the physics underlying the CFPs, to give guidelines for the synthesis of new molecules, optimizing their desired properties. The model of Rinehart and Long based on electrostatic interactions within an axial symmetry has provided successful guidelines.[10] In paramagnetic NMR spectroscopy, Bleaney's theory provides a useful background that allows the contact and dipolar contributions to pNMR shifts to be unraveled,[2] and consequently covalent contributions to be evaluated. This theory is based on CF theory, which reduces to only one CFP for the whole lanthanide series. The aim of this work was to gain more physical insights into CFPs, by evaluating them for two series of lanthanides from first principles.

Ab initio calculations have already been applied successfully to the determination of model Hamiltonian parameters. First-principles approaches enable a full description of the complexity of molecular systems. Ab initio calculations have shown their potential for the determination of model Hamiltonians parameters. This allows the underlying mechanisms to be determined and the loss of information to be evaluated by projecting the whole complexity onto a few parameters. The magnetic coupling constant of the Heisenberg Hamiltonian has been extensively described by both wave-function-based and DFT methods.[56] More recently, ab initio calculations were applied to the calculation of anisotropic magnetic couplings[20,57] and to the ZFS in transition-metal complexes.[21,23]

In this work, to determine the CFPs from ab initio calculations, two recently developed methods were applied to two series of lanthanide complexes. The first series shows very close to D_{4d} symmetry and a compressed environment due to the presence of metallacrowns. The second series displays an approximate three-fold symmetry due to the presence of counter ions and an oblate environment. The description of these molecular systems by ab initio methods allows a description beyond electrostatic interactions and the determination of the 27 CFPs.

This is the first time that the ITO and AILFT methods have been compared. AILFT is based on the fitting of the CF matrix written at the orbital level, whereas the ITO method involves a decomposition of the Hamiltonian matrix for a *J* manifold. These methods lead to very similar CFPs, which confirms that the ZFS occurs mostly at the orbital level, as has been shown previously for lanthanides[31] and for a complex of Ni^{II}.[37] However, small discrepancies between AILFT and ITO reveal many-electron effects on the CFPs: These tend to decrease the CFPs in the first half of the series and to increase them in the second half. When calculating CFPs with one or other method, one should be aware that they do not include the same ingredients. The ITO CFPs are effective and reproduce the energies and composition of a given *J* manifold and are suitable for spectroscopies probing only one *J* manifold, usually magnetic properties. The AILFT CFPs may describe different *J* manifolds, once the spin–orbit coupling and Slater–Condon parameters are known, and this method is consequently suitable for spectroscopies involving different *J* manifolds, such as absorption or emission spectroscopy. Trends were explored by introducing strength parameters, which are rotational invariant. They have been shown to be a very convenient tool for comparing series by reducing the discussion to only one parameter. Strength parameters were introduced for each order and for each index. The latter are not rotational invariant, but they allow for the quantification of rotational symmetry, as for the second series, of three-fold symmetry.

B_0^2 has opposite signs in the two series in accordance with the respective prolate and oblate environments. Because the CFPs are transferable within a series, magnetic properties follow the sign of the pre-factor α_J^2. Because the $LnZn_{16}$ series is axial, B_0^2 is negative, and the magnetization is axial (planar) for erbium (dysprosium). In the second series, because B_0^2 is positive, the opposite trend is expected. Yet, because the sym-

metry is not strictly axial, it is not the case: While the dysprosium complex exhibits an axial magnetization along the pseudo-three-fold axis (as expected), the terbium derivative also exhibits an axial magnetization, in a direction perpendicular to that of the dysprosium complex.

The value of B_0^2 deduced from our calculations is larger than that deduced from the pNMR shifts of the $[Ln(dpa)_3]^{3-}$ series by using Bleaney's theory. This reveals that the B_0^2 of Bleaney's theory is an effective parameter that incorporates other effects. This should be further investigated.

Finally, as expected, the CFPs are transferable along the two series in accordance with Equation (4), in which the reduced parameter α_j^k is related to the metal ion and the B_q^k to the ligands. But they show a systematic decrease across the series, which has already been observed in other series. It has been shown that within a PC model reproducing the electrostatic potential of the ligands, the CFPs are rather constant across the series; it has been shown to arise from a counterbalance between the shrinking of the coordination sphere and the greater compactness of the 4f orbitals. The decrease in the CFPs across the series is consequently attributed to covalent effects, defined as all effects beyond electrostatic interactions. They comprise bonding, charge-transfer, and polarization effects. They are not restricted to the overlap of the 4f and ligand orbitals. Covalent bonding mostly occurs through the more outer-shell orbitals, that is, the 6s and 5d orbitals; the change in the electron density of the lanthanide center affects the splitting of the 4f orbitals, and thus the CFPs.

Computational Details

For all the investigated systems, calculations were performed on the crystallographic structures by using the SO-CASSCF (spin–orbit-complete active space self-consistent field) approach. MOLCAS calculations were performed with the MOLCAS (version 7.8) suite of programs.[58] Firstly, a SF-CASSCF (spin-free CASSCF) calculation was performed[59] with an active space composed of the seven 4f orbitals of the lanthanide ion and associated electrons, that is, CAS(*n*,7). Spin–orbit (SO) coupling was included by a state interaction with the RASSI (restricted active space state interaction) method.[60] All the spin states with the highest value of *S* and 27 singlets (Pr, Tm), 43 doublets (Nd, Er), 86 quartets (Sm), 42 quintets (Eu, Tb), 108 quartets (Dy), 99 triplets (Ho), 35 quartets (Er), or 2 triplets (Tm) were considered for the state interaction. Scalar relativistic effects were taken into account by means of the Douglas–Kroll–Hess transformation,[61] and the SO integrals were calculated by using the AMFI (atomic mean-field integrals) approximation.[62] For the $LnZn_{16}$ series, the lanthanide and coordinating NO was described by a TZP ANO-RCC basis, atoms of the first cycle of the 12-MC-4 sandwiches with a DZP basis, and the most remote atoms with SZ. 24-MC-8 was described by point charges and zinc by effective core potentials (ECPs) with 1s 1p.[63] For $TbZn_{16}$, $DyZn_{16}$, and $ErZn_{16}$, $LnZn_{16}(picHA)_{16}$ structures were considered.[25] For $HoZn_{16}$, calculations were performed on both the structures of the neighboring-ion derivatives, dysprosium and erbium, and averaged afterwards. For $YbZn_{16}$, the $YbZn_{16}(pizHA)_{16}$ complex was considered.[26] For the $[Ln(dpa)_3]^{3-}$ series, the lanthanide and the O, N, C, and H atoms were described with the ANO-RCC basis sets of QZP and TZP quality, respectively. The *g* factors were calculated according to Ref. [64] and the CFPs were calculated with a local program written in Mathematica.

All the ORCA-SO-CASSCF calculations were performed by using the ORCA 4.0 quantum chemistry package.[65] For the CASSCF calculations, the default CI setting (i.e., CSFCI) was used in combination with the SuperCI and then NR settings for the orbital step. Scalar relativistic effects were accounted for by using the second-order scalar relativistic Douglas–Kroll–Hess (DKH2) Hamiltonian formalism.[66,67] SO coupling was then accounted for in a mean-field fashion (SOMF) by using quasi-degenerate perturbation theory (QDPT)[68] and allowing all CASSCF (SO-free) states from all spin multiplicities to mix through the SOMF operator. To facilitate this task, the CASSCF (SO-free) states were determined by using a state-average approach, with all CASSCF states equally weighted.

All-electron scalar relativistic SARC2-QZVP basis sets[69] were used for the lanthanide atoms and the DEF2-QZVPP basis set[70,71] for the other atoms (i.e., H, C, N, and O). The present DEF2-TZVPP basis sets are an adapted version of the DEF2 basis set from the Karlsruhe group (i.e., Ahlrichs basis set), which is provided in the Turbomole basis set library. They retain the original DEF2 exponents but with contraction coefficients suitable for the DKH scalar relativistic Hamiltonian. Finally, the AUTOAUX feature[72] was used to automatically generate auxiliary basis sets for the resolution of identity approximation (RI-JK),[73] which helps speed up the calculations.

Acknowledgements

This work was supported by the ANR under convention No. ANR-17-CE06-0010. This work was sponsored by the US DOE through the LANL. LANL is operated by Triad National Security, LLC, for the NNSA of the US DOE (Contract No. 89233218NCA000001). J.J. thanks LANL for funding through a Director's Postdoctoral fellowship. This work was supported by the National Science Foundation under grant CHE-1361799 to V.L.P.

Conflict of interest

The authors declare no conflict of interest.

Keywords: ab initio calculations · crystal field theory · lanthanides · magnetic properties

[1] R. Sessoli, A. K. Powell, *Coord. Chem. Rev.* **2009**, *253*, 2328 – 2341.
[2] B. Bleaney, *J. Magn. Reson. (1969)* **1972**, *8*, 91.
[3] H. Bethe, *Ann. Phys.* **1929**, *395*, 133.
[4] J. H. Van Vleck, *J. Chem. Phys.* **1935**, *3*, 807.
[5] G. Racah, *Phys. Rev.* **1949**, *76*, 1352.
[6] K. W. H. Stevens, *Proc. Phys. Soc. London Sect. A* **1952**, *65*, 209.
[7] B. G. Wybourne, *Spectroscopic Properties of Rare Earths*, Wiley, New York, **1965**.
[8] H. Schilder, H. Lueken, *J. Magn. Magn. Mater.* **2004**, *281*, 17 – 26.
[9] N. F. Chilton, R. P. Anderson, L. D. Turner, A. Soncini, K. S. Murray, *J. Comput. Chem.* **2013**, *34*, 1164 – 1175.
[10] J. D. Rinehart, J. R. Long, *Chem. Sci.* **2011**, *2*, 2078 – 2085.
[11] J. J. Baldovì, J. J. Borrás-Almenar, J. M. ClementeJuan, E. Coronado, A. Gaita-Arino, *Dalton Trans.* **2012**, *41*, 13705.
[12] J. J. Baldovì, J. M. Clemente-Juan, E. Coronado, A. Gaita-Arino, *Inorg. Chem.* **2014**, *53*, 11323 – 11327.

[13] G. Huang, G. Fernandez-Garcia, I. Badiane, M. Camarra, S. Freslon, O. Guillou, C. Daiguebonne, F. Totti, O. Cador, T. Guizouarn, B. Le Guennic, K. Bernot, *Chem. Eur. J.* **2018**, *24*, 6983 – 6991.
[14] N. F. Chilton, D. Collison, E. J. L. McInnes, R. E. P. Winpenny, A. Soncini, *Nat. Commun.* **2013**, *4*, 2551.
[15] G. R. Choppin, *Pure Appl. Chem.* **2002**, *27*, 23 – 42.
[16] G. R. Choppin, *J. Alloys Compd.* **2002**, *344*, 55 – 59.
[17] M. L. Neidig, D. L. Clark, R. L. Martin, *Coord. Chem. Rev.* **2013**, *257*, 394 – 406.
[18] T. Gupta, M. K. Singh, G. Rajaraman in *Topics in Organometallic Chemistry*, Springer, Berlin, **2018**, pp. 1 – 74.
[19] L. Ungur in *Lanthanide-Based Multifunctional Materials, Advanced Nanomaterials* (Eds.: P. Martín-Ramos, M. Ramos Silva), Elsevier, Amsterdam, **2018**, pp. 1 – 58.
[20] F. Gendron, J. Autschbach, J. Malrieu, H. Bolvin, *Inorg. Chem.* **2019**, *58*, 581 – 593.
[21] L. Chibotaru, L. Ungur, *J. Chem. Phys.* **2012**, *137*, 064112.
[22] H. Bolvin, J. Autschbach in *Handbook of Relativistic Quantum Chemistry* (Ed.: W. Liu), Springer, Berlin, **2017**, pp. 725 – 763.
[23] R. Maurice, R. Bastardis, C. de Graaf, N. Suaud, T. Mallah, N. Guihéry, *J. Chem. Theory Comput.* **2009**, *5*, 2977.
[24] F. P. Notter, H. Bolvin, *J. Chem. Phys.* **2009**, *130*, 184310.
[25] J. Jankolovits, C. M. Andolina, J. W. Kampf, K. N. Raymond, V. L. Pecoraro, *Angew. Chem. Int. Ed.* **2011**, *50*, 9660 – 9664; *Angew. Chem.* **2011**, *123*, 9834 – 9838.
[26] I. Martinic, S. V. Eliseeva, T. N. Nguyen, V. L. Pecoraro, S. Petoud, *J. Am. Chem. Soc.* **2017**, *139*, 8388 – 8391.
[27] J. W. Kampf, T. Mallah, V. L. Pecoraro, private communication.
[28] M. Autillo, L. Guerin, T. Dumas, M. S. Grigoriev, A. M. Fedoseev, S. Cammeli, P. L. Solari, P. Guilbaud, P. Moisy, H. Bolvin, C. Berthon, *Chem. Eur. J.* **2019**, *25*, 4435.
[29] M. Atanasov, D. Aravena, E. Suturina, E. Bill, D. Maganas, F. Neese, *Coord. Chem. Rev.* **2015**, *289*, 177.
[30] L. Ungur, L. F. Chibotaru, *Chem. Eur. J.* **2017**, *23*, 3708 – 3718.
[31] R. Alessandri, H. Zulfikri, J. Autschbach, H. Bolvin, *Chem. Eur. J.* **2018**, *24*, 5538 – 5550.
[32] A. Abragam, B. Bleaney, *Electronic Paramagnetic Resonance of Transition Ions*, Clarendon, Oxford, **1970**.
[33] C. Görller-Walrand, K. Binnemans in *Handbook on the Physics and Chemistry of Rare Earths, Vol. 23* (Eds.: K. A. Gschneidner, Jr., L. Eyring), Elsevier, Amsterdam, **1996**, Chapter 155.
[34] C. Rudowicz, J. Qin, *Phys. Rev. B* **2003**, *67*, 174420.
[35] N. C. Chang, J. B. Gruber, R. P. Leavitt, C. A. Morrison, *J. Chem. Phys.* **1982**, *76*, 3877 – 3889.
[36] Y. Y. Yeung in *Crystal Field Handbook* (Eds.: D. J. Newman, B. K. C. Ng), Cambridge University Press, Cambridge, **2000**, pp. 160 – 175.
[37] G. Charron, E. Malkin, G. Rogez, L. J. Batchelor, S. Mazerat, R. Guillot, N. Guihéry, A. L. Barra, T. Mallah, H. Bolvin, *Chem. Eur. J.* **2016**, *22*, 16850 – 16860.
[38] L. Chibotaru, A. Ceulemans, H. Bolvin, *Phys. Rev. Lett.* **2008**, *101*, 033003.
[39] D. P. Hernández, H. Bolvin, *J. Electron Spectrosc. Relat. Phenom.* **2014**, *194*, 74.
[40] K. Lea, M. Leask, W. Wolf, *J. Phys. Chem. Solids* **1962**, *23*, 1381.
[41] M. Atanasov, C. A. Daul, C. Rauzy in *Optical Spectra and Chemical Bonding in Inorganic Compounds: Special Volume Dedicated to Professor Jørgensen I* (Eds.: D. M. P. Mingos, T. Schönherr), Springer, Berlin, **2004**, pp. 97 – 125.
[42] M. Atanasov, J. M. Zadrozny, J. R. Long, F. Neese, *Chem. Sci.* **2013**, *4*, 139 – 156.
[43] D. Aravena, M. Atanasov, F. Neese, *Inorg. Chem.* **2016**, *55*, 4457 – 4469.
[44] J. Jung, M. Atanasov, F. Neese, *Inorg. Chem.* **2017**, *56*, 8802 – 8816.
[45] J. S. Griffith, *The Theory of Transition Metal Ions*, Cambridge University Press, Cambridge, **1961**.
[46] R. N. Zare, *Angular Momentum*, Wiley, New York, **1988**.
[47] W. Van den Heuvel, A. Soncini, *J. Chem. Phys.* **2013**, *138*, 054113.
[48] C. Y. Chow, H. Bolvin, V. E. Campbell, R. Guillot, J. W. Kampf, W. Wernsdorfer, F. Gendron, J. Autschbach, V. Pecoraro, T. Mallah, *Chem. Sci.* **2015**, *6*, 4148.
[49] P. Zhang, J. Jung, L. Zhang, J. Tang, B. Le Guennic, *Inorg. Chem.* **2016**, *55*, 1905 – 1911.
[50] L. Gagliardi, R. Lindh, G. Karlström, *J. Chem. Phys.* **2004**, *121*, 4494 – 4500.
[51] C.-K. Duan, P. A. Tanner, *J. Phys. Chem. A* **2010**, *114*, 6055 – 6062.
[52] T. R. Faulkner, J. P. Morley, F. S. Richardson, R. W. Schwartz, *Mol. Phys.* **1980**, *40*, 1481 – 1488.
[53] N. Ishikawa, M. Sugita, T. Okubo, N. Tanaka, T. Iino, Y. Kaizu, *Inorg. Chem.* **2003**, *42*, 2440 – 2446.
[54] C. N. Reilley, B. W. Good, J. F. Desreux, *Anal. Chem.* **1975**, *47*, 2110 – 2116.
[55] M. Vonci, K. Mason, E. A. Suturina, A. T. Frawley, S. G. Worswick, I. Kuprov, D. Parker, E. J. L. McInnes, N. F. Chilton, *J. Am. Chem. Soc.* **2017**, *139*, 14166 – 14172.
[56] P. de Loth, P. Cassoux, J. P. Daudey, J. P. Malrieu, *J. Am. Chem. Soc.* **1981**, *103*, 4007.
[57] R. Ruamps, R. Maurice, C. de Graaf, N. Guihiéry, *Inorg. Chem.* **2014**, *53*, 4508 – 4516.
[58] F. Aquilante, L. De Vico, N. Ferré, G. Ghigo, P.-A. Malmqvist, P. Neogrády, T. B. Pedersen, M. Pitonak, M. Reiher, B. Roos, M. SerranoAndrés, M. Urban, V. Veryazov, R. Lindh, *J. Comput. Chem.* **2010**, *31*, 224.
[59] B. O. Roos, P. R. Taylor, P. E. M. Siegbahn, *Chem. Phys.* **1980**, *48*, 157.
[60] P.-A. Malmqvist, B. O. Roos, B. Schimmelpfennig, *Chem. Phys. Lett.* **2002**, *357*, 230.
[61] B. A. Hess, *Phys. Rev. A* **1986**, *33*, 3742.
[62] B. A. Hess, C. M. Marian, U. Wahlgren, O. Gropen, *Chem. Phys. Lett.* **1996**, *251*, 365.
[63] S. López-Moraza, J. L. Pascual, Z. Barandiarán, *J. Chem. Phys.* **1995**, *103*, 2117 – 2125.
[64] H. Bolvin, *ChemPhysChem* **2006**, *7*, 1575.
[65] F. Neese, *WIREs Computational Molecular Science* **2018**, *8*, e1327.
[66] M. Reiher, *Theor. Chem. Acc.* **2006**, *116*, 241 – 252.
[67] T. Nakajima, K. Hirao, *Chem. Rev.* **2012**, *112*, 385 – 402.
[68] F. Neese, *J. Chem. Phys.* **2005**, *122*, 034107.
[69] D. Aravena, F. Neese, D. A. Pantazis, *J. Chem. Theory Comput.* **2016**, *12*, 1148 – 1156.
[70] F. Weigend, F. Furche, R. Ahlrichs, *J. Chem. Phys.* **2003**, *119*, 12753 – 12762.
[71] F. Weigend, R. Ahlrichs, *Phys. Chem. Chem. Phys.* **2005**, *7*, 3297 – 3305.
[72] G. L. Stoychev, A. A. Auer, F. Neese, *J. Chem. Theory Comput.* **2017**, *13*, 554 – 562.
[73] F. Neese, *J. Comput. Chem.* **2003**, *24*, 1740 – 1747.

Manuscript received: July 10, 2019
Revised manuscript received: August 28, 2019
Accepted manuscript online: September 9, 2019
Version of record online: October 30, 2019